


Article

Stress-Relief–Anchor-Grouting, a Collaborative Control Technology for Severe Extrusion Floor Heave in a Deep Roadway: A Case Study

Donghuang Shang¹, Meng Wang^{1,2,*} , Dawei Li^{1,2}, Chunsheng Yu³, Shiyi Huang¹, Jie Li⁴, Sijiang Wei^{1,2} and Liuan Zhao³

¹ School of Energy Science and Engineering, Henan Polytechnic University, Jiaozuo 454000, China

² State Collaborative Innovation Center of Coal Work Safety and Clean-Efficiency Utilization, Jiaozuo 454003, China

³ Henan Energy Chemical Group Co., Ltd., Guhanshan Coal Mine, Jiaozuo 450046, China; Zla_ghs@126.com (L.Z.)

⁴ Ejin Holo Banner Energy Administration, Ordos 017000, China; lj_rise@126.com

* Correspondence: mengwang@hpu.edu.cn

Abstract: Severe extrusion floor heave is the most common type of failure of floors in deep roadways, and it is also a major problem restricting the safe and efficient mining of deep coal resources. In deep roadways, reducing floor stress is an effective means to control floor heave. In this study, the method of creating directional stress-relief zones by constructing stress-relief boreholes is applied; while the stress is released, the path of stress from the ribs transferred to the floor and to the extrusion failure path is cut off, and floor heave control is achieved. Therefore, based on the stress-boundary and rock-mass parameters of the roadway, the control effects of the borehole angle, length, diameter, and row spacing on the extrusion floor heave were studied, and the reasonable thresholds of borehole parameters were shown to ensure the stress-relief effect on the roadway. In addition, the bolt-grouting technology was used to strengthen the floor of the roadway, the broken surrounding rock was modified via grouting consolidation, the support strength of the floor was increased using high-tension bolts (cable), and there was a good floor heave control effect in the field application. On the basis of traditional floor reinforcement, the control effect of stress regulation on floor heave is fully considered in this study, and stress-relief–anchor-grouting, a collaborative control technology for floor heave in deep roadways, is developed. Based on the three factors affecting the stability of deep roadways (stress, lithology, and support), the collaborative prevention and control of severe extrusion floor heave were realized, which provides a new method for deep roadway floor heave control and has good application value.



Citation: Shang, D.; Wang, M.; Li, D.; Yu, C.; Huang, S.; Li, J.; Wei, S.; Zhao, L. Stress-Relief–Anchor-Grouting, a Collaborative Control Technology for Severe Extrusion Floor Heave in a Deep Roadway: A Case Study. *Sustainability* **2023**, *15*, 13053. <https://doi.org/10.3390/su151713053>

Academic Editors: Deyu Qian and Zhiyi Zhang

Received: 14 July 2023

Revised: 19 August 2023

Accepted: 21 August 2023

Published: 30 August 2023



Copyright: © 2023 by the authors. Licensee MDPI, Basel, Switzerland. This article is an open access article distributed under the terms and conditions of the Creative Commons Attribution (CC BY) license (<https://creativecommons.org/licenses/by/4.0/>).

Keywords: deep roadway; extrusion floor heave; borehole stress relief; anchor grouting support; collaborative control

1. Introduction

The intensification of coal mining has caused the depletion of shallow coal resources in many mining areas in China, and coal mining has been transferred to deeper levels [1–3]. Under the strong influence of deep stress, the structure, behaviors, characteristics, and engineering response of coal and rock masses have undergone fundamental changes. Large, nonlinear deformation and continuous rheology occur easily after roadway excavation, especially due to floor heave [4,5]. It has been found that more than 70% of the roof and floor movement of roadways without floor support is due to floor heave, and the amount of roadway maintenance caused by floor heave accounts for more than 50% of the total amount [6]. Therefore, the prevention and control of floor heave have become the focus and challenge of deep roadway control.

In order to solve the problem of floor heave in deep roadways, domestic and foreign scholars have put forward much research regarding the mechanisms, influencing factors, and treatment methods of floor heave and have achieved fruitful results. Sungsoon Mo et al. [7–9] pointed out that horizontal stress is the main factor inducing roadway floor heave and proposed a classification method for roadway floors based on studies of floor heave mechanisms. Hongpu Kang [10] and Qingwen Zhu et al. [11] found that rock stratum bending, dilatancy, and dilation are the main causes of floor heave in roadways and pointed out that the stress relief method is an effective means to prevent and control floor heave. Yaodong Jiang [12], S.B. Tang [13], and Tie Wang et al. [14], based on an analysis of the factors influencing floor heave, classified floor heave into four categories: extrusion flow type, flexural fold type, shear dislocation type, and water expansion type. Manchao He [15], Weijun Wang [16,17], and Yong Chen et al. [18] proposed a control method for floor heave using the interaction among the roof, ribs, and floor, revealing the action mechanism of roof relief, inventing a bolt net and cable-coupled support to control floor heave. Jianbiao Bai [19,20], Ying Xu [21], and Yiming Zhao et al. [22] revealed the “two points and three zones” feature of floor-heave roadways under dynamic stress, developing floor steel-pile and U-shaped steel-sealing supports, which achieved a good control effect for floor heave by optimizing the roadway layout and strengthening the broken floor. Renshu Yang [23,24], Xiaoming Sun [25–27], Meng Wang [28], and Zhiqiang Wang et al. [29] studied the characteristics of weakly consolidated laminar floors and asymmetric floor heave with gob-side entry and developed the stress regulation of misaligned roadway layouts and the differentiated zoning control of a high-strength anchor to grout floors. Jingyi Cheng et al. [30] clarified the coupling triggering mechanism of floor heave stress extrusion and hydraulic weakening in deep soft rock roadways and developed a combined floor-heave-control technology for grouting reinforcement based on floor-blasting stress relief. Lihui Sun [31], Xiaoqing Wang [32], Jiong Wang [33], and Qingliang Chang et al. [34] developed a floor heave joint control scheme including a floor cable bunch + deep and shallow grouting, inverted floor arch + bolts, and a hydraulic dilation anchor rod, achieving effective floor heave control effects in field tests.

The existing research on floor heave control can be categorized into three aspects—stress manipulation, surrounding rock modification, and support strengthening—among which the latter two are paid more attention. However, it has been found that there is difficulty in obtaining a satisfactory control effect from the modification and reinforcement of surrounding rock through field applications, and the relative reduction in the surrounding rock stress is fundamental to maintaining floor stability [35]. Nowadays, the common floor heave control methods for deep roadways include optimizing the roadway layout [36], excavating stress-relief roadways [37], loosening blasting [38], slotting in the floor [39], etc. Among them, optimizing the roadway layout and excavating stress-relief roadways concern stress-relief technologies outside the roadways and include negative factors such as a large amount of engineering and high cost, and they have been replaced by loosening blasting and slotting in the floor and other stress-relief technologies inside the roadways [40]. The stress-relief technologies inside the roadways include building artificial crushing zones, which effectively alleviate the high stress accumulation and severe extrusion effect of the floor and then reduce the deformation of the floor [41]. However, the key to the popularization and application of this technology is not the control effect but the safety and efficiency aspects. For instance, many mining areas are subject to the influences of explosive materials and mine safety protection, and there is no condition for loose blasting. However, slotting in the floor has the negative aspects of high cost, high labor intensity, and high construction difficulty.

In recent years, borehole stress-relief technology has gradually become the mainstream stress-transfer method in roadways due to its advantages of its simple process, convenient construction, and low cost [42], and it has been widely applied in the fields of dynamic disaster prevention and control [43], high-stress roadway control [44], and gas seam antireflection [45]. The problems in floor heave control in typical deep, high-stress roadways

are addressed in this study, with a focus on exploring the weakening control effect of stress-relief boreholes on severe extrusion floor heave and developing the collaborative control technology of stress-relief–anchor-grouting in deep roadway floor heave, which provides a new method for floor heave control and ensures the safe and efficient production of deep mines.

2. Field Background

2.1. Mine Introduction

The coal mine of Henan Energy Chemical Group Co., Ltd., Guhanshan, was used as the field background. Gas-extraction roadway #1605 was selected as the test roadway; it is the roadway ensuring the safety of longwall face #1605, and it was used to construct the gas-extraction borehole of the 21# coal seam. As shown in Figure 1, the test roadway is buried about 795 m deep, with a total length of 1661.8 m, and it is located 12 m below the floor of the 21# coal seam. In order to ensure that the roof and ribs of the test roadway are stable, the test roadway is arranged in a siltstone layer, and the floor of the test roadway is located in a sandy mudstone layer with low strength. For details, see the red box zone of the borehole column section in the lower-right corner of Figure 1.

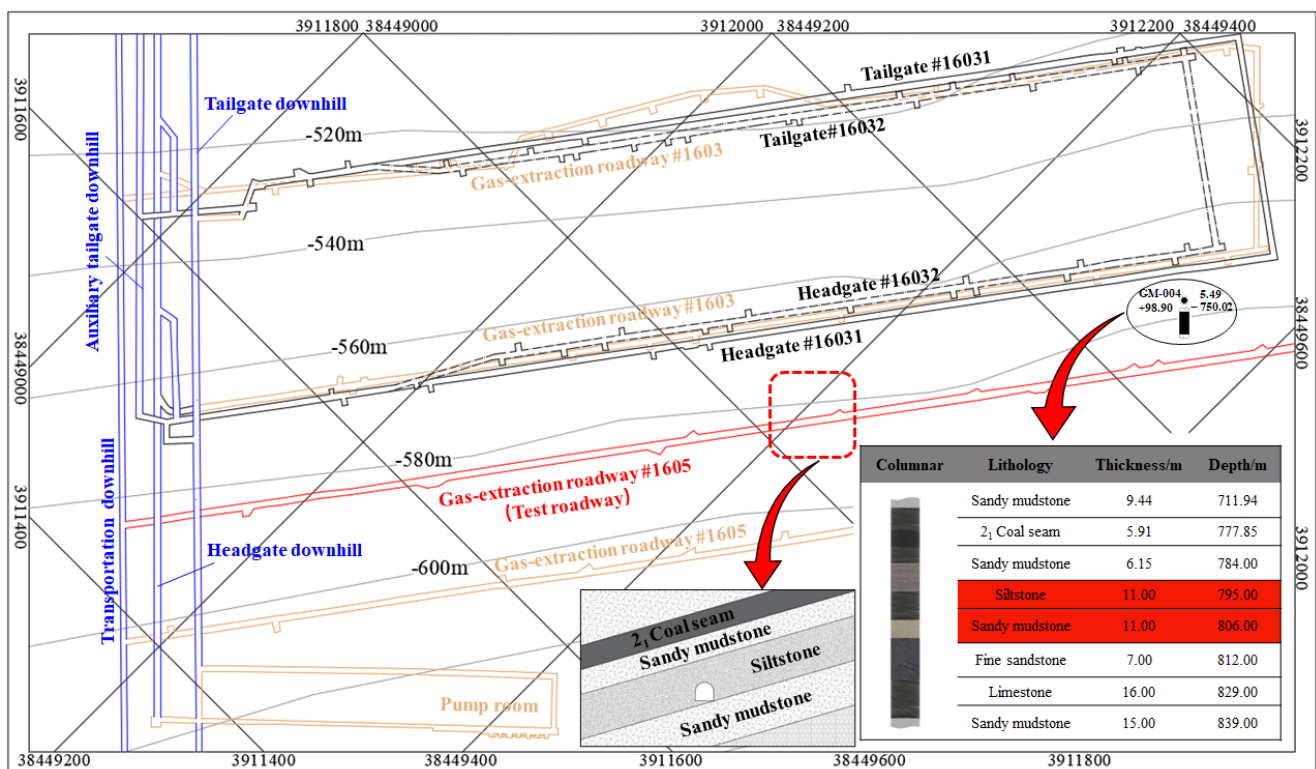


Figure 1. Mine excavation plan.

As shown in Figure 2, the test roadway is a straight wall with a semi-circular arch and a size (width × height) of 4.5 m × 4.5 m, and it consists of combined bolting with wire mesh and a cable. The anchor bolt specification is $\Phi 20$ mm × L2400 mm, and the spacing row is 800 mm × 800 mm. Anchor cable support is applied to the roof to strengthen the support. The anchor cable specification is a $\Phi 18.9$ mm × L7500 mm high-strength prestressed anchor cable, and the spacing rows are 1600 mm × 1600 mm, with three cables in each row. A metal net of $\Phi 6$ mm is laid between the anchor rod (cable) and the roadway surface, and the mesh is 70 mm × 70 mm. After the roof support was completed, shotcrete was used to seal the spray layer, with a thickness of 50 mm. It should be pointed out that there is no effective support for the floor in the test roadway.

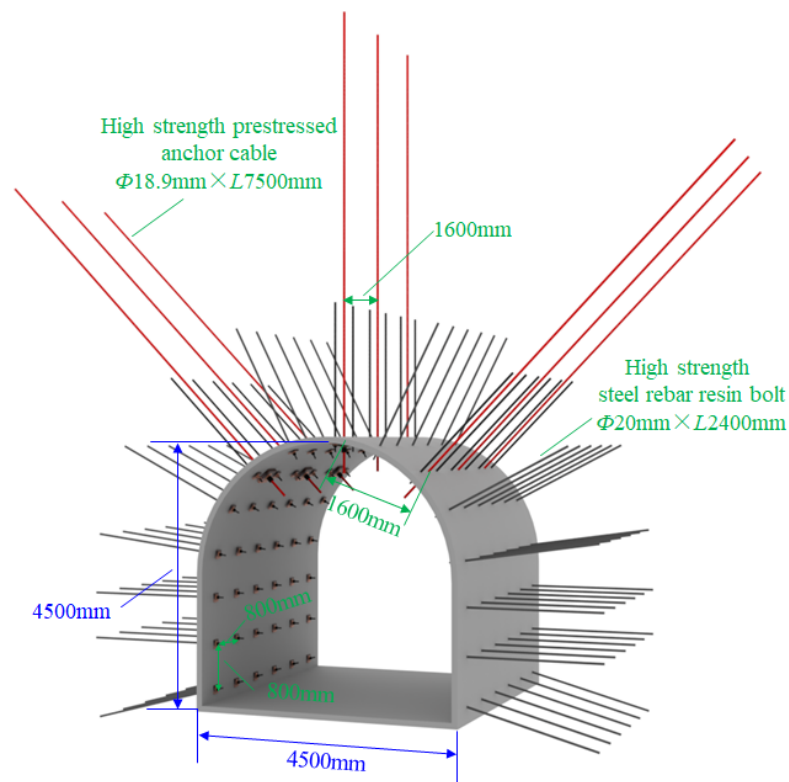


Figure 2. Test roadway's original support.

2.2. Severe Extrusion Floor Heave in Deep Roadways

Photos of the pumping lane of the test roadway are shown in Figure 3. It can be seen from the figure that after roadway support is added, the deformation of the roof can be effectively controlled, and the deformation of the floor heave increases. The severe extrusion flow failure is shown in the floor, and the maximum floor heave of the roadway is 1 m, which leads to the inclination, rollover, and distortion of the floor track and induces a local slope, which severely affects the normal use of the roadway. According to the mining and excavating relationship between the longwall face and the roadways seen in Figure 1, when floor heave occurs in the test roadway, the coal seam above it is not mined, and the roadway is in the initial stress environment. An in situ stress test was carried out on the area near the test roadway, and the measured location is shown with the red dot in Figure 1. The hollow inclusion strain method was adopted for the in situ stress measured; a total of three measuring points were arranged, and the results show that the area near the test roadway is dominated by horizontal stress, as shown in Table 1. Through the coordinate transformation of the in situ stress test results, the ratio of horizontal stress to vertical stress (side stress coefficient) of the test roadway is about 1.3, which aligns with the value of a typical roadway affected by tectonic stress.

The results indicate that the maximum principal stress after the excavation of the roadway in a horizontal stress field is mainly concentrated in the interior of the roof and floor, which produces extrusion in the surrounding rock [46]. If the floor is not supported or the engineering disturbance is severe, strong extrusion floor heave may be induced in the roadway under the action of horizontal stress. There is a directly proportional relationship between floor heave and the side stress coefficient [47]. As the side stress coefficient becomes larger, the quantity of floor heave increases linearly. With the failure and unloading of the floor, the accumulated vertical stress in the two ribs is transferred to the floor along the bottom angle and released, which induces the intensification of the heave extrusion flow behavior on the floor. As shown in Figure 4, the long-term extrusion

deformation of the floor will loosen the two ribs and roof of the roadway and induce overall disaster and roadway instability in severe cases.



Figure 3. Photos of test roadway.

Table 1. In situ stress test results.

	Value/MPa	Azimuth/°	Dip Angle/(°)
Maximum principal stress (σ_1)	36.17	194.51	42.63
Intermediate principal stress (σ_2)	23.08	119.86	−39.56
Minimum principal stress (σ_3)	19.25	262.21	−15.93
In situ stress component	σ_X /MPa	σ_Y /MPa	σ_Z /MPa
	24.91	34.44	19.25

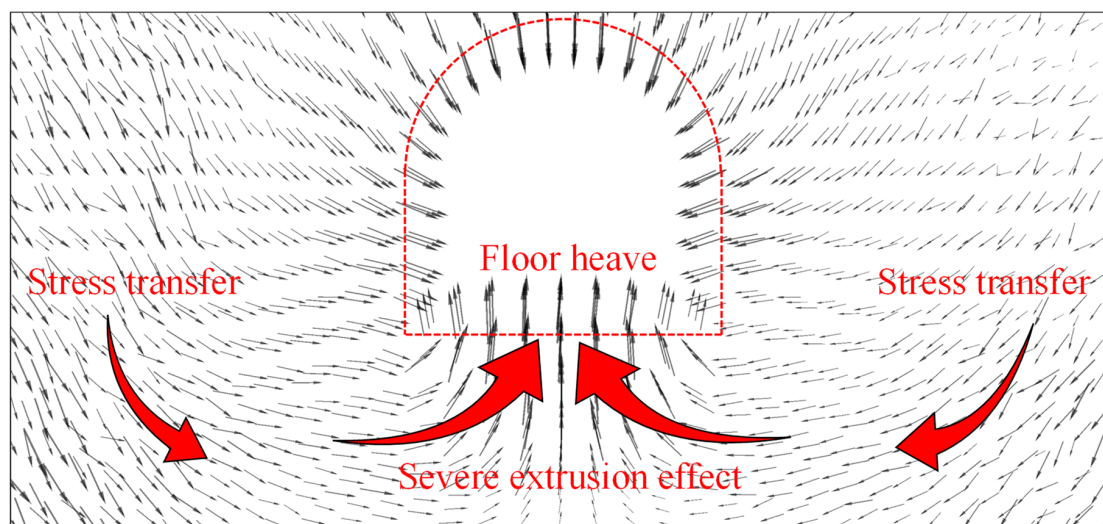


Figure 4. Floor extrusion deformation.

Extrusion-flowing floor heave is the most common and recognized type of floor heave in deep roadways [48]. Researchers have fully understood the mechanism of this type of floor heave and have developed control technologies such as strengthening the roof, constructing the bottom angle, adding a floor anchor (cable), and relieving the stress [49–51]. Based on existing research results, this study poses a beneficial attempt at deep extrusion

floor heave collaborative control using the regulation of floor stress environment and floor reinforcement. The overall research idea of the study is shown in Figure 5.

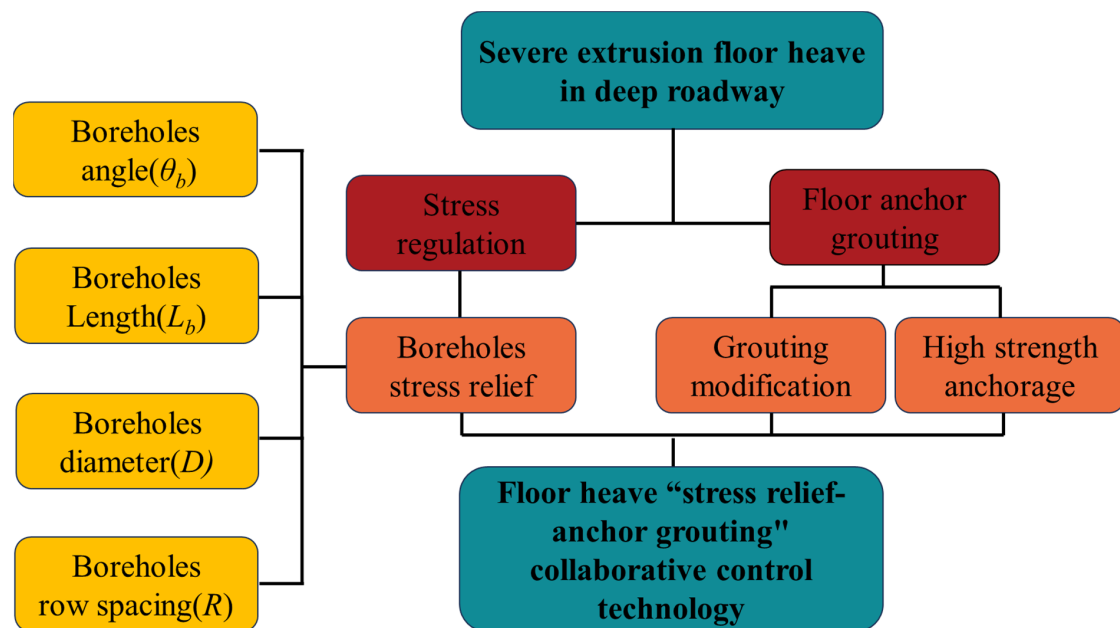


Figure 5. Analysis flowchart.

3. Principle and Technology of Floor-Heave-Relief Weakening Control

3.1. Stress-Relief Control Principle of Floor Heave Boreholes

The continuous extrusion of surrounding rock induced by floor failure is the main reason for severe floor heave in deep roadways [47]. If the stress-relief method is adopted to cut off the stress and the flow direction of the fractured rock mass and improve the stress environment of the floor, the degree of floor heave can be significantly reduced [52]. To address the disadvantages of commonly used stress-relief techniques such as loosening blasting and slotting in the floor, this study introduces borehole stress-relief technology for floor heave control engineering.

According to the borehole stress-relief principle [53], there are two functions of the construction of stress-relief boreholes. One is to form an artificial crushing zone along the roadway via the superposition of the plastic zone adjacent to the boreholes, cutting off the transfer path of the stress on the roadway ribs and broken rock mass to the floor, and improving the floor stress environment, as shown in Figure 6b. The other is to use the boreholes' space to provide compensation space for the volume dilation deformation of the roadway's surrounding rock and reduce the radial displacement of the roadway, as shown in Figure 6c.

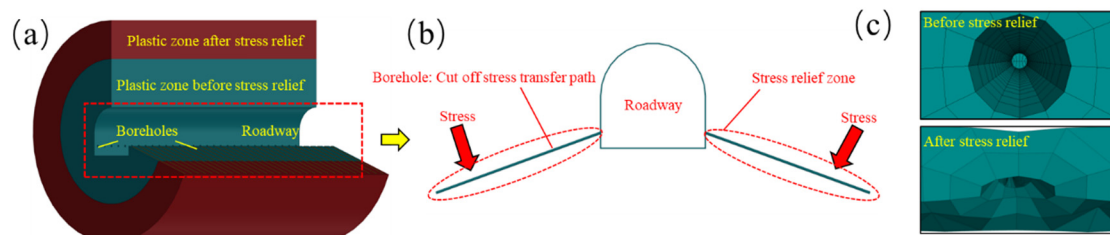


Figure 6. Borehole stress-relief control principle. (a)—Effect of stress relief boreholes on plastic zone; (b)—The stress transfer path is cut off by stress relief boreholes; (c)—Compensation space caused by stress relief boreholes.

Research shows that the stress-relief effect of the roadway is mainly affected by the borehole parameters, but there is no theoretical basis for determining the borehole parameters. The authors and the research and development team have made some efforts and attempts to design stress-relief borehole parameters, and it is clearly pointed out in the literature [42] that the orientation, length, diameter, and row distance of the borehole directly affect the stress transfer and deformation control effect of the roadway. Therefore, based on the previous research results, the control effect of the above key drilling parameters on the roadway floor heave will be discussed.

3.2. Numerical Analysis Model

The three-dimensional numerical model of the test roadway was established, as shown in Figure 7. The mesh generation, division, and grouping of the model in the early stages were completed using HyperMesh2019 software, and the model was imported into FLAC3D6.0 software through the conversion interface. The model includes different angles θ_b (0° , 10° , 20° , 30° , 40° , and 50°) and different diameters D (100 mm, 200 mm, 300 mm, 400 mm, and 500 mm). The center distance of the boreholes is 1 m, which makes 1 m, 2 m, ..., n m, and other integer row spacings possible for borehole construction. Considering the internal correlation between the borehole diameter and the row spacing [54], the ratio of the borehole diameter D to the row spacing R (D/R) was adopted as the index to analyze and determine the layout density of the boreholes. The size of the numerical model was $X \times Y \times Z = 60 \text{ m} \times 16 \text{ m} \times 60 \text{ m}$. The displacement of the horizontal and bottom boundaries of the model was fixed. The constitutive of the model is strain softening, and the stress boundary condition was applied to the upper boundary and the horizontal direction according to the in situ test results, in which a 19.25 MPa vertical stress was applied to the upper boundary, 24.91 Mpa was applied in the horizontal X direction, and 34.44 Mpa was applied in the Y direction.

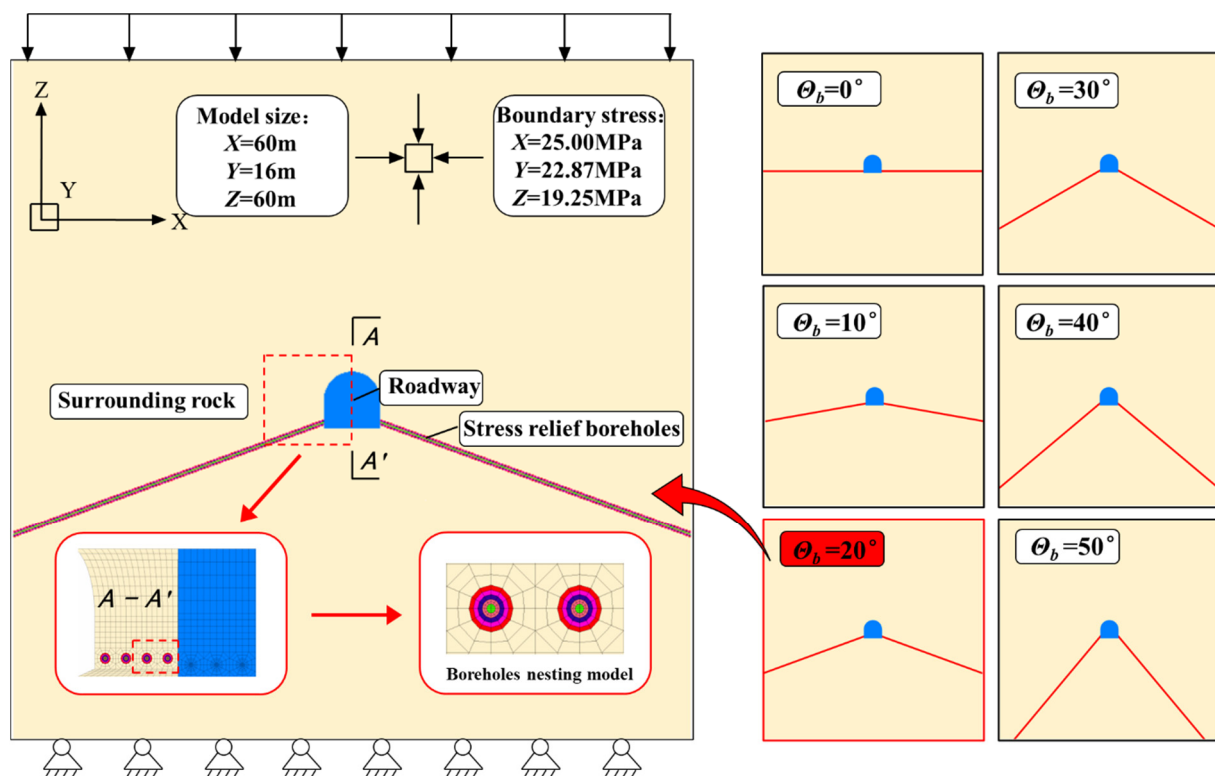


Figure 7. Numerical model diagram.

The floor's rock samples were obtained via borehole coring, and the rocks' physical and mechanical parameters were tested in the laboratory, as shown in the second row of

Table 2. The research object was the generation mechanism and prevention of floor heave. For the sake of simplification, the changes in the conditions of rock strata occurrence were ignored in the established model, and to assign parameters to the model globally, a floor made of sandy mudstone was adopted.

Table 2. Physical and mechanical parameters.

	Category	Density/(kg/m ³)		Elasticity Modulus/GPa	Poisson	c ₀ /MPa		φ ₀ (°)	Tensile Strength /MPa	
Pre-peak parameters	Laboratory experiment	3663		10.26	0.31	4.41		28.5	1.14	
	Inverse modeling	3663		2.57	0.31	3.26		28.3	0.35	
Post-peak softening parameters	Plastic parameter ε ^{ps}	0	0.001	0.002	0.003	0.004	0.005	0.01	0.1	1
	c _{ε^{ps}} /MPa	3.26	2.34	1.74	1.35	1.11	0.95	0.70	0.67	0.67
	φ _{ε^{ps}} /°	28.3	23.3	21.0	19.9	19.5	19.3	19.1	19.1	19.1

The post-peak softening property of the rock material was also considered: the attenuation of the post-peak parameters of coal samples should be considered in the numerical simulation; otherwise, it is difficult to accurately describe the total stress–strain and yield–failure behaviors of coal samples [55]. It was found that the rock mass cohesion c and the internal friction angle φ changed with the increase in plastic strain ε^{ps} . In numerical analyses, the post-peak softening characteristics of the rock mass are often simulated by establishing the functional relationship between c , φ , and ε^{ps} [56]. In the literature [42], the function expressions of c , φ , and ε^{ps} are established using laboratory loading and unloading experiments. After parameters are normalized, the post-peak parameters of the rock mass can be calculated according to Equation (1):

$$\begin{cases} c_{\varepsilon^{ps}}/c_0 = 0.799e^{-\varepsilon^{ps}/0.00225} + 0.205 \\ \varphi_{\varepsilon^{ps}}/\varphi_0 = 0.328e^{-\varepsilon^{ps}/0.00123} + 0.676 \end{cases} \quad (1)$$

where c_0 and φ_0 are the initial cohesion and internal friction angle of coal samples, MPa, (°), and $c_{\varepsilon^{ps}}$ and $\varphi_{\varepsilon^{ps}}$ are the cohesion force and internal friction angle corresponding to the plastic strain ε^{ps} MPa, (°).

RocLab1.0 software was used to convert the rock sample parameters obtained through the experiment into rock mass parameters [57], and the attenuation law of c and φ with ε^{ps} were obtained using Equation (1). The field-measured roadway deformation was taken as the target value, and the numerical simulation parameters of the rock mass were inverted using the iterative method. The verification process is shown in Figure 8; the curve in the figure is the result of numerical simulation, and the scatter is the result of field measurement. The initial parameters of the rock mass obtained through inversion are shown in row 3 of Table 2, and the parameters of the post-peak softening of the rock mass are shown in the last three rows of Table 2.

3.3. Key Technical Parameters Determination of Borehole Stress Relief

The research indicates that the main factors affecting the stress-relief effect of the boreholes are the stress-relief orientation, the stress-relief parameters, etc. [58]. Then, the established model and the parameters of inversion were used to study the control effect of the borehole stress relief on the compressive floor heave of the test roadway, which provides a theoretical basis for the determination of stress-relief parameters and field tests.

Based on a literature search and on the basis of the previous research [59], two indices of stress regulation and deformation control were selected to analyze the effect of roadway stress relief, with a total of four variables: the failure depth of the floor (d_f), the floor heave (δ_f), the horizontal peak stress (σ_m), and the distance between the horizontal peak stress and the floor (l_f).

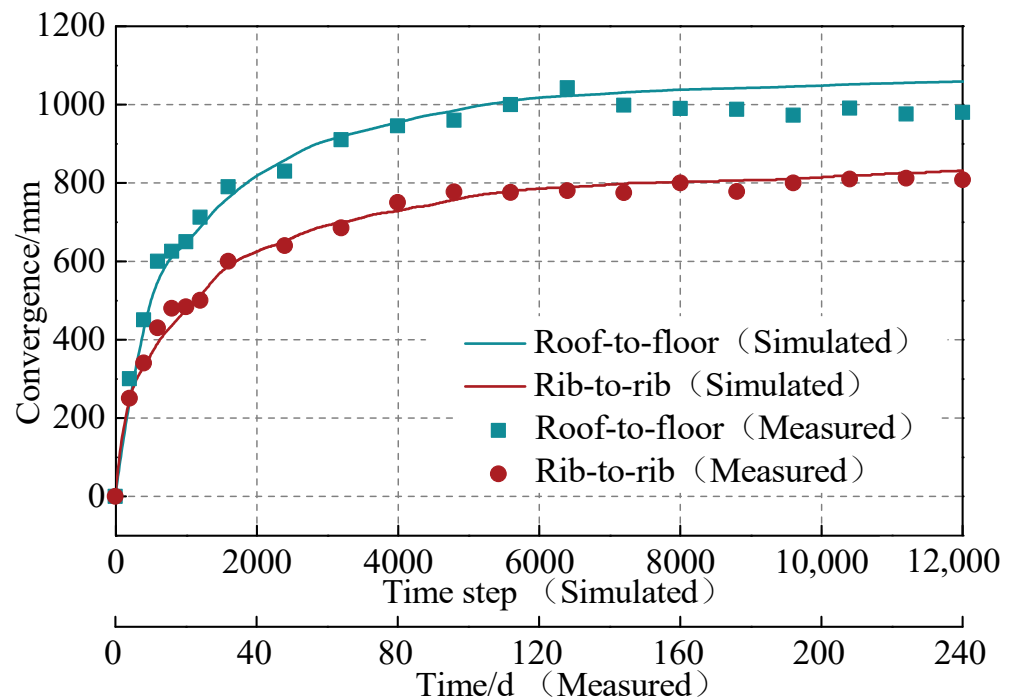


Figure 8. Numerical simulation parameters validation.

3.3.1. Borehole Angle θ_b

Cutting off the release of high stress along the floor is an effective method to control the extrusion floor heave. The construction position of the stress-relief boreholes is generally in two ribs or the floor, and it is more common to use two ribs for the stress-relief boreholes, because there are defects in the construction of floor boreholes, such as difficulty in discharging slag and low efficiency [60]. The construction boreholes in roadway ribs is taken as an example: the effect of stress regulation and floor heave control on roadway floors was studied by adjusting the boreholes' angle.

During the simulation, the boreholes' diameter D was fixed at 500 mm; the length L_b was 14 m; the row distance R was 1 m; the angle θ_b was taken as the independent variable; and 0° , 10° , 20° , 30° , 40° , and 50° were taken as the comparison models. Figure 9 shows the relationship curves between d_f , δ_f , σ_m , and l_f and the borehole θ_b . As can be seen in Figure 9, the construction of stress-relief boreholes is conducive to the control of floor heave. When θ_b is in the range of 0° to 40° , d_f and δ_f decrease as a whole with the increase in θ_b . From the perspective of stress analysis, the regulation effect of floor stress is different with the increase in θ_b . Specifically, when $\theta_b \in [0^\circ, 20^\circ]$, the effect on the floor stress concentration area is limited, and when $\theta_b > 20^\circ$, the σ_m and l_f show a decreasing trend.

It should be noted that when $\theta_b > 40^\circ$, the effect of floor stress regulation and floor heave control slows down. In addition, the increase in θ_b has more and more stringent requirements for drilling machine performance, resulting in a significant increase in the difficulty of borehole construction. For the test roadway, the borehole angle should reasonably be controlled within the range of 20° – 40° . The horizontal stress, vertical displacement, and roadway failure nephograms without boreholes and with borehole angles of 20° and 40° are shown in Figure 10. It can clearly be seen from the figure that stress-relief boreholes have barrier effects on the floor stress distribution and displacement transfer, and the construction of stress-relief boreholes can effectively reduce the failure depth and floor heave.

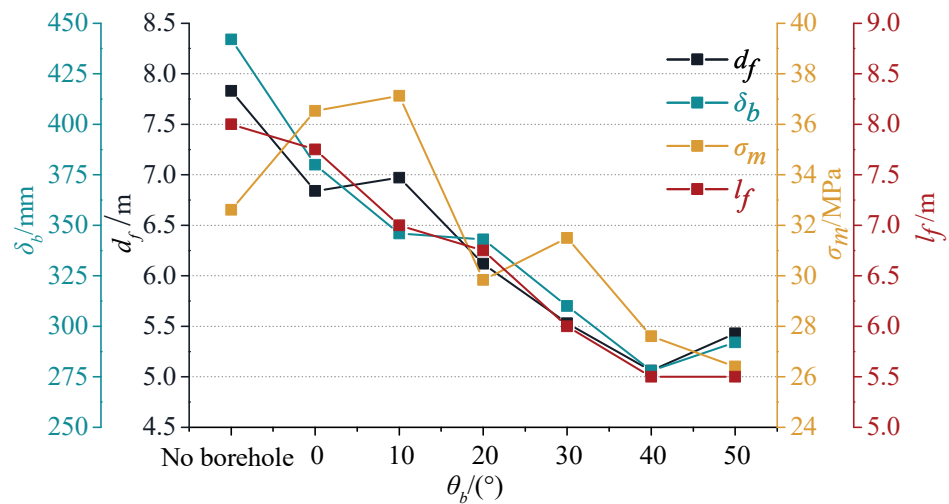


Figure 9. The relationship between d_f , δ_b , σ_m , and θ_b .

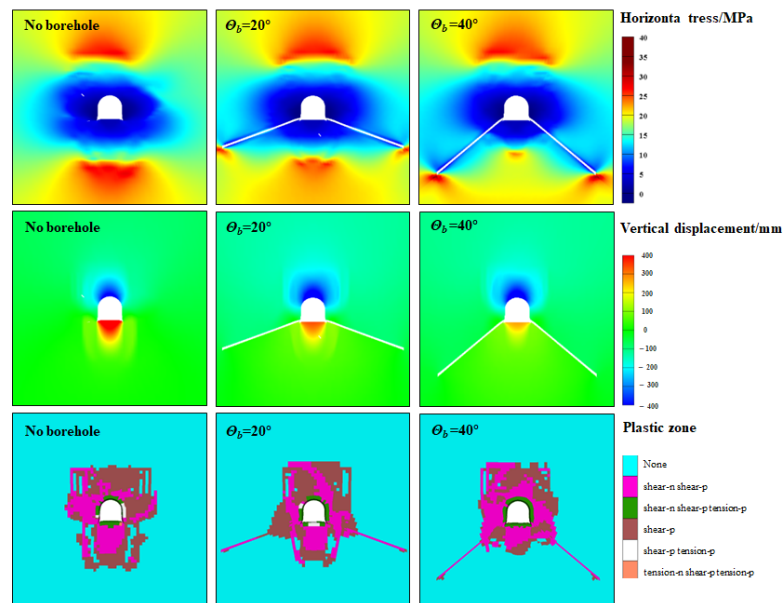


Figure 10. Simulation nephograms.

3.3.2. Borehole Length L_b

The length of the stress-relief boreholes L_b was analyzed with a θ_b of 20° , a D of 500 mm, and an R of 1 m. The relationship curves of d_f , δ_b , σ_m , and l_f with L_b are shown in Figure 11. It can be seen from the figure that with the increase in L_b , the stress concentration degree of the floor is effectively alleviated, σ_m decreases, and d_f gradually decreases. When $L_b > 14$ m, σ_m , l_f , and d_f gradually become stable.

With the increase in L_b , δ_b first decreases and then increases. The inflection point emerges at position $L_b = 8$ m and then δ_b increases slowly with L_b . As shown in Figure 12, the deformation trend in the roadway ribs is the same as that of the floor, but that of the roof is different. With the increase in L_b , the roof deformation shows a linear growth trend, which is mainly caused by the overall subsidence of the roof caused by the extension of the crushing zone of the boreholes. In the field, when determining L_b , factors such as stress regulation, floor heave, and roof subsidence should be taken into consideration, and the balance of multiple factors should be studied. For the test mine, from the perspective of floor heave control, the borehole length should not be less than 8 m. From the perspective of stress regulation and construction quantity, the borehole length should not exceed 14 m.

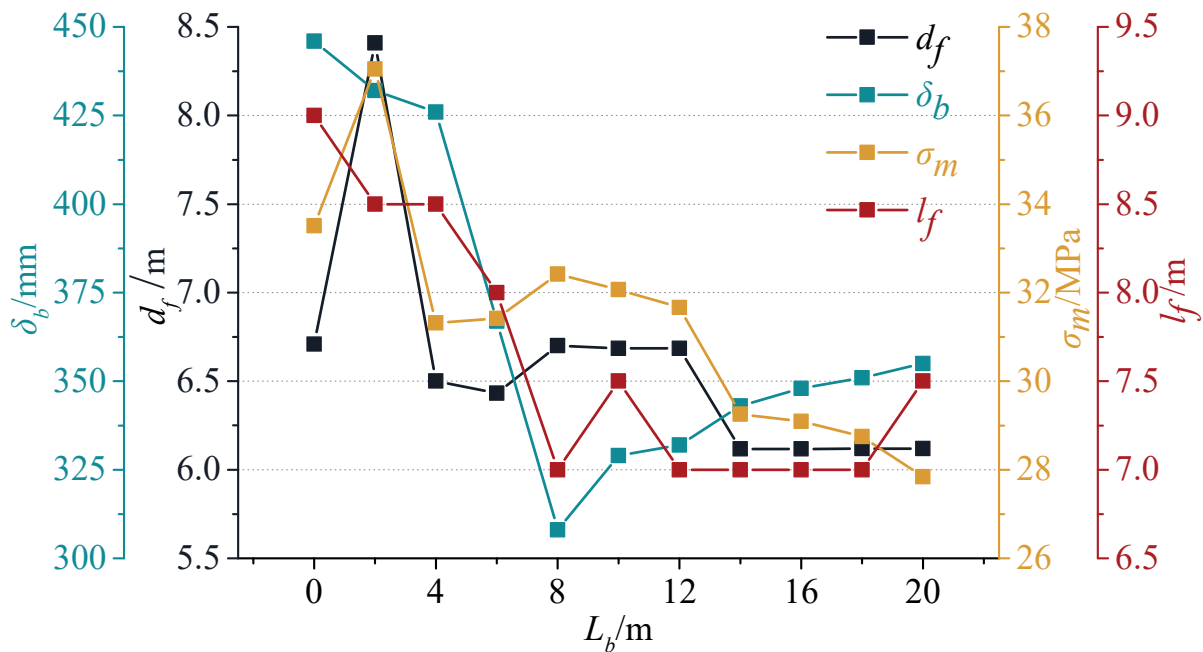


Figure 11. The relationship between floor stress, displacement, and borehole length.

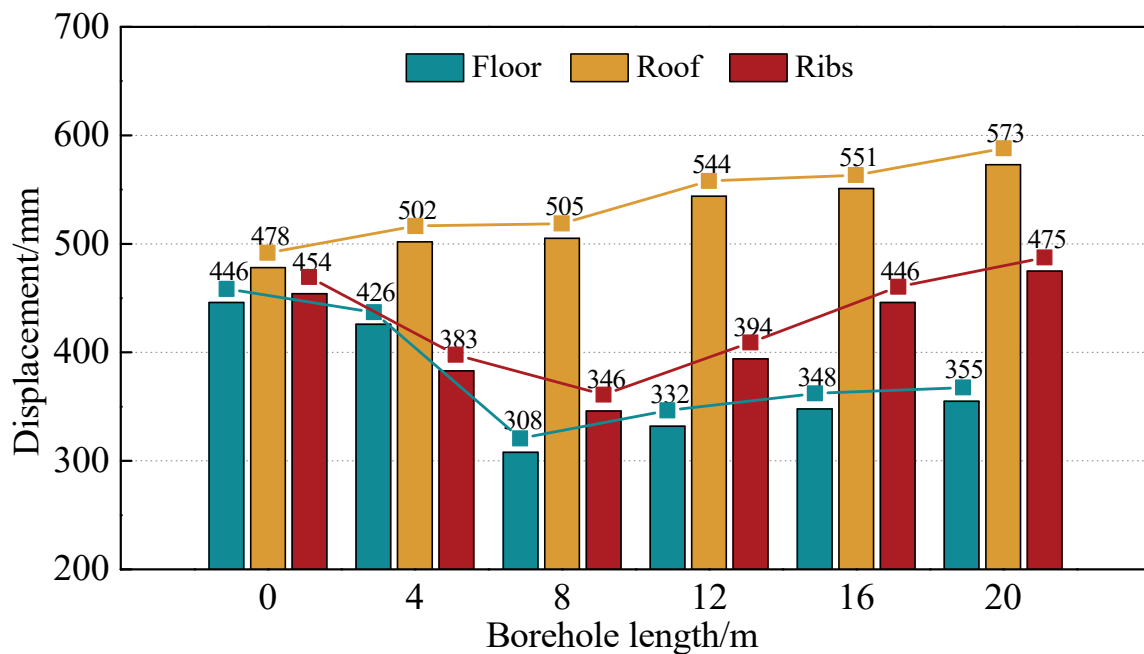


Figure 12. The deformation of surrounding rock varies with the length of the boreholes.

3.3.3. Borehole Diameter D and Row Spacing R

The results show that the borehole diameter D and row spacing R are two variables that influence each other [54]. With the increase in D , R can be appropriately increased and vice versa. Therefore, the ratio of D/R is selected as a variable to comprehensively study the influence of D and R on floor heave control.

Figure 13 shows the relationship curves of d_f , δ_b , σ_m , l_f , and D/R . As can be seen from the figure, with the increase in D/R , the greater the degree of breakage of the surrounding rock (Figure 13 (the upper right panel)), the better the barrier effect on the stress transfer, and σ_m and l_f decrease. The bigger the D/R , the smaller the degree of damage to the roadway floor, which can be proved by the linear attenuation relationship between the floor

deformation and the floor deformation depth with D/R . However, it should be noted that a bigger D/R is not always better. When the D/R is greater than $1/2$, the rock mass along the stress relief area can easily lose its bearing capacity. At this time, the row of boreholes is similar to the slotting along the direction of the roadway, which causes the overall subsidence of the roof under the action of self-weighted stress, which is very unfavorable for roadway maintenance. For the test roadway, a reasonable D/R is less than or equal to $1/2$.

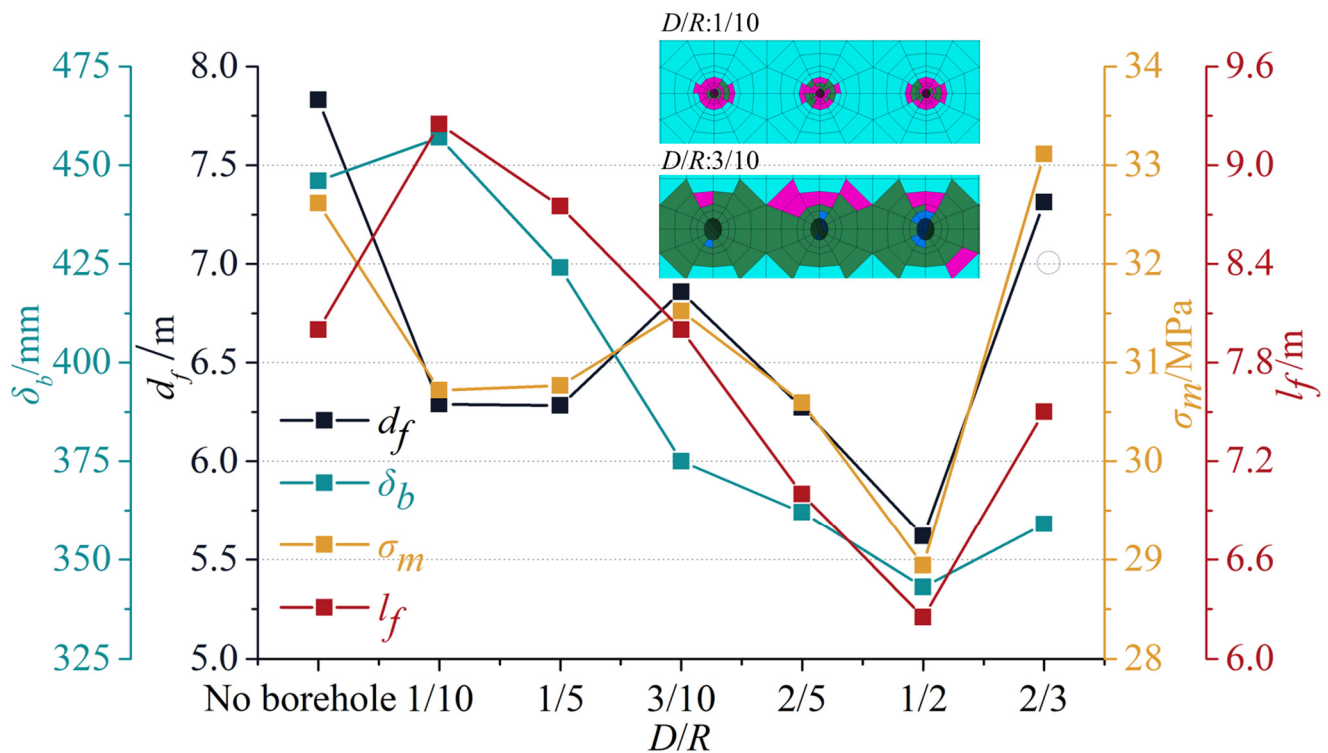


Figure 13. The relationship between stress, displacement of the floor, and D/R .

4. Floor Heave Stress-Relief-Anchor-Grouting Collaborative Control Technology

4.1. Principle of Anchor Grouting Support for Roadway Floors

Similar to the support from the roof and two ribs, roadway floor support can also be divided into initiative support (bolt, cable, anchor grouting, etc.) [31–34,61] and passive support (U-shaped steel, poured concrete, etc.) [21,22]. However, it is worth emphasizing that whether it is a newly excavated roadway or a repaired roadway, the inverted arch should be excavated before the floor is supported, as shown in Figure 14, for two reasons. Firstly, the inverted arch can peel off the shallow broken floor and increase the effect of the initiative and passive support (Figure 14b). Secondly, it can seal the tail of the bolt (cable) or U-shaped steel in the inverted arch by means of pouring concrete (Figure 14c) so as not to affect the use of the roadway.

Influenced by the difficulty of construction and the effect of the support, the method of strengthening the floor with U-shaped steel is gradually being replaced by initiative support methods such as bolt (cable) or anchor grouting [62]. At present, the anchor-grouting support method to reinforce the floor is common. In order to improve the efficiency of excavation, many mines only pay attention to the roof support and then deal with damage after severe floor heave occurs, and in this situation, the floor is composed of loose, broken surrounding rock. For the anchor grouting support, grouting can be used to block the broken surrounding rock, improve the strength and integrity of the surrounding rock, and provide a reliable foundation for the application of high prestress on the bolt (cable).



Figure 14. Inverted arch in the roadway.

In this section, the collaborative control effect of anchor grouting support and borehole stress relief on floor heave is studied by taking anchor grouting reinforcement for the floor as an example. As shown in Table 3, three schemes were set during the analysis: (1) no roadway-control technology, (2) borehole stress relief, and (3) borehole stress relief + anchor grouting. Before the simulation analysis, it was necessary to clarify the strengthening effect of anchor-grouting support on the mechanical parameters of the broken surrounding rock. In the literature [35], the functional relationship between rock mechanics parameters and support strength was obtained using a similar laboratory simulation test method. For the test roadway, a Mohr–Coulomb model was assigned as the constitution model in the anchorage zone, the support strength of 0.35 MPa was taken as an example, and through the conversion of rock mass strength, the mechanical parameters shown in Table 4 were used to assign parameters to the floor anchoring area to simulate the anchor grouting support.

Table 3. Modeling schemes.

Scheme	Borehole Stress Relief	Anchor Grouting Support	Borehole Stress-Relief Parameters				Anchor Grouting Support Parameters
			$\theta_b/(\circ)$	L_b/m	D/m	R/m	Strength/MPa
1	No	No					
2	Yes	No					
3	Yes	Yes	20	14	0.5	1	0.35

Table 4. Simulated support parameters.

Support Intensity P_i/MPa	Density/(kg/m^3)	Elasticity Modulus/GPa	Poisson	c_0/MPa	$\varphi_0/(\circ)$	Tensile Strength/MPa
0.35	3663	3.855	0.31	1.005	28.65	0.35

The stress and deformation data of the roadway's surrounding rock corresponding to the three schemes are shown in Figure 15. It can be seen from the figure that the anchor-grouting support on the floor after the stress relief can effectively reduce the stress concentration of the surrounding rock of the floor and reduce the failure range and deformation of the floor. It should be pointed out, as shown in Figure 16, that when the floor is reinforced with anchor grouting, the roof deformation can be improved at the same time to make up for the roof and ribs additional deformation caused by the stress relief, playing a role of strengthening the floor and controlling the roof.

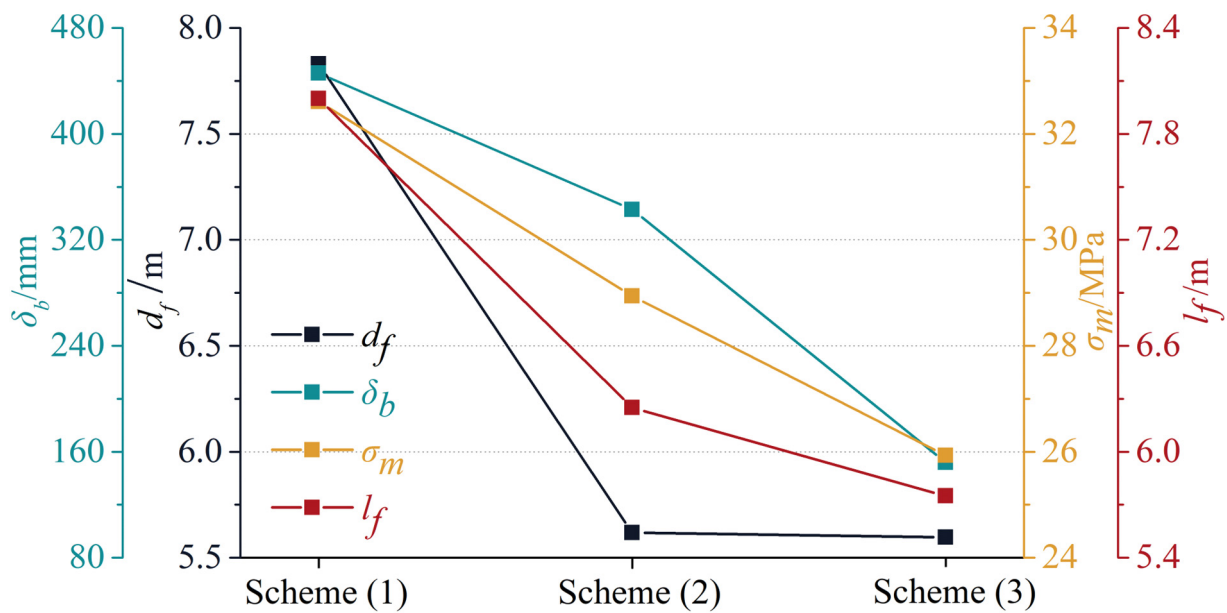


Figure 15. Influence of different schemes on roadway stress and displacement.

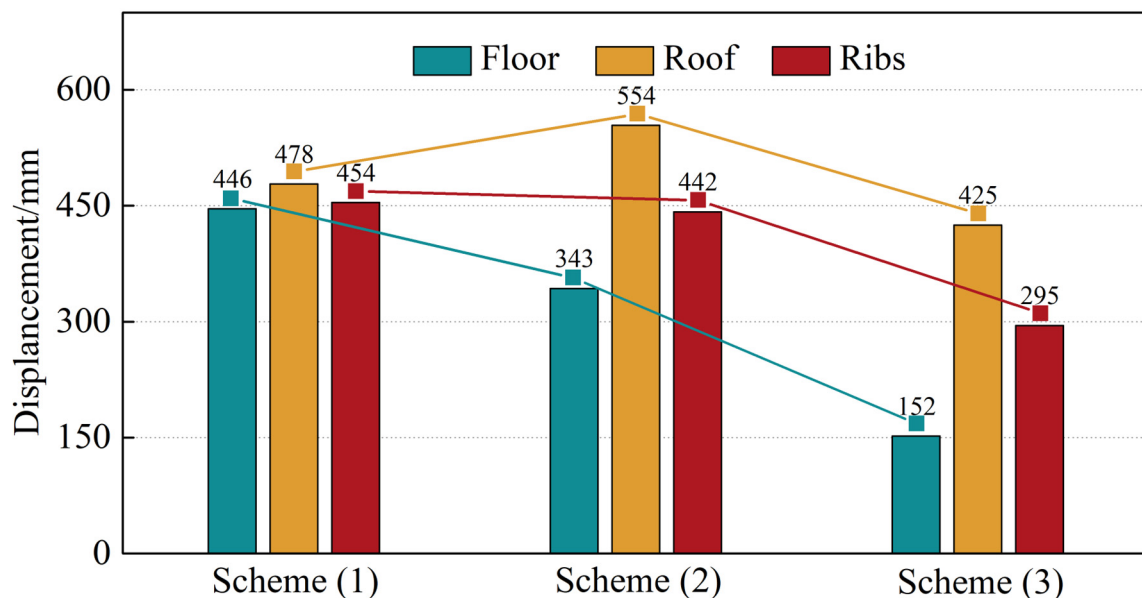


Figure 16. Variation in surrounding rock deformation under different schemes.

4.2. Floor Heave Stress-Relief-Anchor-Grouting, a Collaborative Control Technology

4.2.1. Confirmation of Key Parameters

Based on the above results, the severe extrusion floor heave stress-relief-anchor-grouting, a collaborative control technology, is proposed. In addition, the field industrial test was finished; the specific test path and parameters were as follows:

(1) Borehole stress relief on the ribs. According to the numerical analysis in Section 3.3, the borehole parameters that can ensure full stress relief of the roadway are as follows: I. θ_b : 20~40°; II L_b : 8~14 m; and III D/R : less than or equal to 1/2. The amount of construction and the difficulty of slagging are considered, the optimal borehole angle θ_b is 20°, and the borehole length L_b is 14 m. It should be pointed out that D/R was finally chosen to be 1/3, and the upper limit of the recommended value of 1/2 was not adopted; the design is

conservative because if the stress relief is excessive, the roof will sink. The drilling machine diameter of the Guhanshan mine is 113 mm, and the final borehole row spacing is 350 mm.

(2) Anchor grouting support for the floor. The test roadway floor heave is severe, and the damage depth is large, resulting in the bolt (cable) losing the anchor strength foundation, and it is difficult to obtain ideal results using the bolt and cable support. To this end, the floor support of the test roadway is reinforced using grouting bolts (cable). Both the grouting bolts and the grouting cable have hollow structures, as shown in Figure 17. The two major processes of grouting and anchoring are integrated, and the functions of the modification of the broken surrounding rock and high-strength anchoring are included.

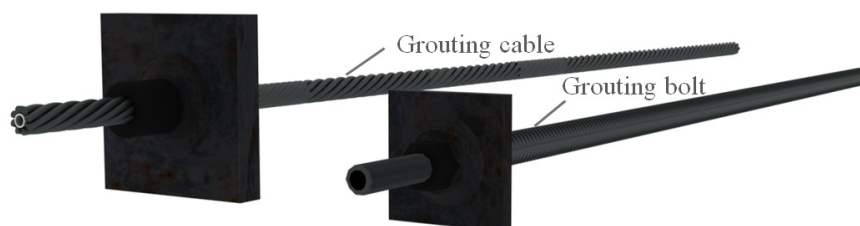


Figure 17. Grouting bolt (cable).

The design of the grouting bolt refers to the conventional design method of the bolt, and the expression of the bolt support strength is presented in the literature:

$$p = \frac{\sigma_t \pi d^2}{4n_1 n_2} \quad (2)$$

where p is the strength of the bolt support, MPa; σ_t is the tensile strength of the bolt material, MPa; d is the bolt diameter, mm; and n_1 and n_2 are the bolt spacing and the row spacing, respectively, mm.

According to Equation (2), when the support strength of the bolt support is 0.35 MPa, with a yield strength of the bolt of 600 MPa as an example, the row spacing between bolts is 900 mm × 900 mm.

The field measurement and numerical simulation show that the failure depth of the floor exceeds the anchoring range of the bolts. In order to effectively control the overall foundation of the anchoring area of the floor, the grouting cable is used to replace the bolts in the special position of the middle and bottom angle of the floor to increase the anchoring depth and avoid the overall extrusion of the anchoring area.

(3) Floor crack seal. After the anchor grouting is completed, in order to increase the integrity of the floor and reduce the engineering disturbance and the weakening effect of the water texture, the backfill is carried out by pouring concrete, and the backfill thickness is about 300 mm.

4.2.2. Field Construction Schemes

The test roadway is the gas-extraction roadway #1605; its field construction process and key technical parameters are shown in Figure 18.

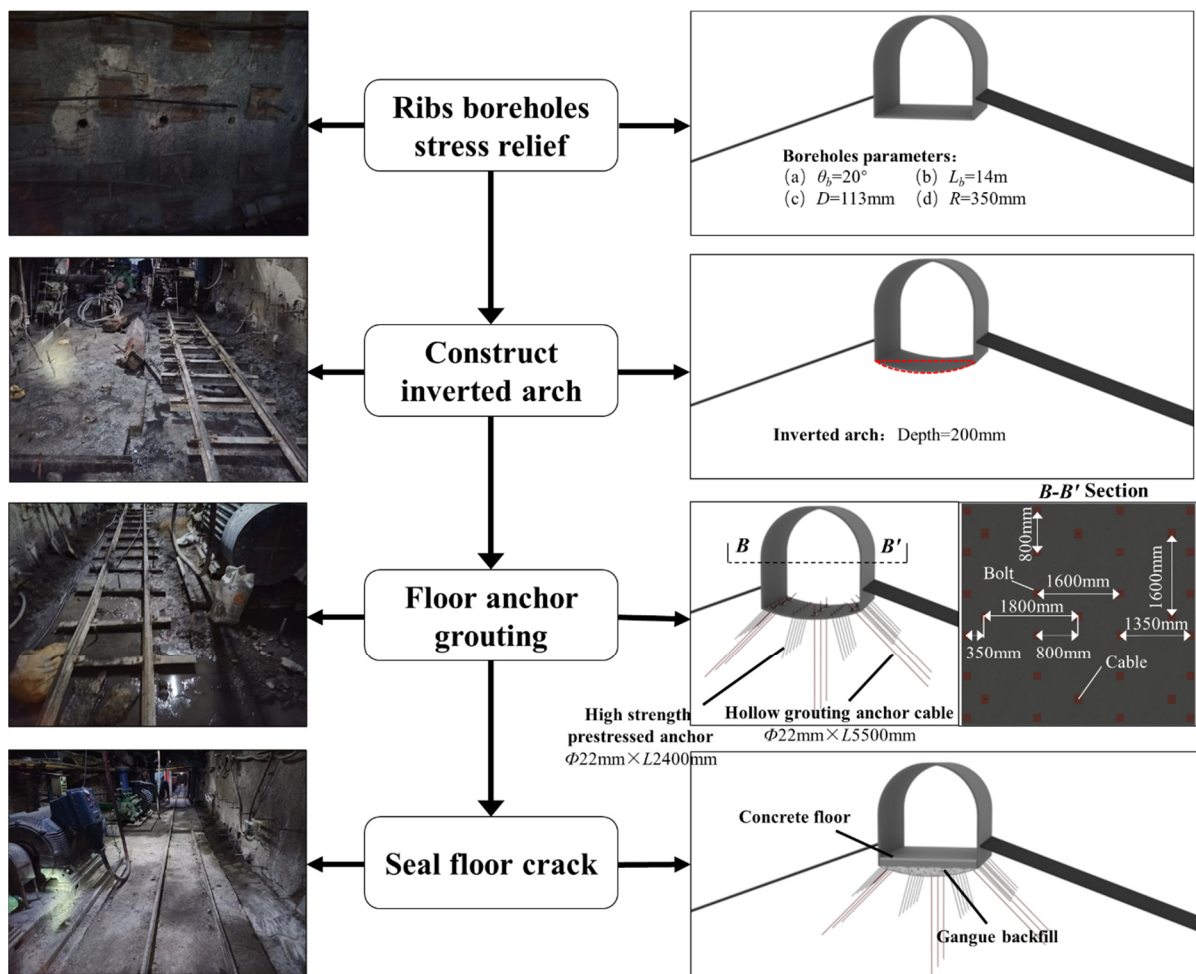


Figure 18. Field construction process and key technical parameters.

5. Field Application Effect

The control technology and parameters presented in Section 4.2 were used for the test roadway; then, the mine stress data were monitored, and the control effect of the floor heave was tested. The monitoring data of the borehole failure, deep roadway rib displacement, floor cable stress, and floor heave are shown in Figures 19–21.

(1) Borehole failure and deep displacement of roadway ribs. After the construction of the stress-relief boreholes, borehole imaging was used to observe the deformation and failure of the boreholes. The images of the borehole ribs after the borehole construction are shown in Figure 19a. A large number of cracks can be seen in the surrounding rock of the roadway ribs, and there are phenomena of local borehole collapse and hole blocking, indicating that the stress-relief effect is good. In order to effectively monitor the stability of the surrounding rock at different depths of the roadway ribs, multi-base point displacement meters were installed 0.5 m above the stress-relief boreholes of the roadway ribs, as shown in Figure 19b. Four measuring points were set 2 m, 4 m, 6 m, and 8 m away from the surface of the roadway ribs, and the monitoring data are shown in Figure 19c. There was no obvious change in the deformation of the surrounding rock at different depths before and after the stress relief, which indicates that the selection of stress-relief borehole parameters is reasonable, and the construction of stress-relief boreholes will not cause instability in the surrounding rock of the ribs and roof.

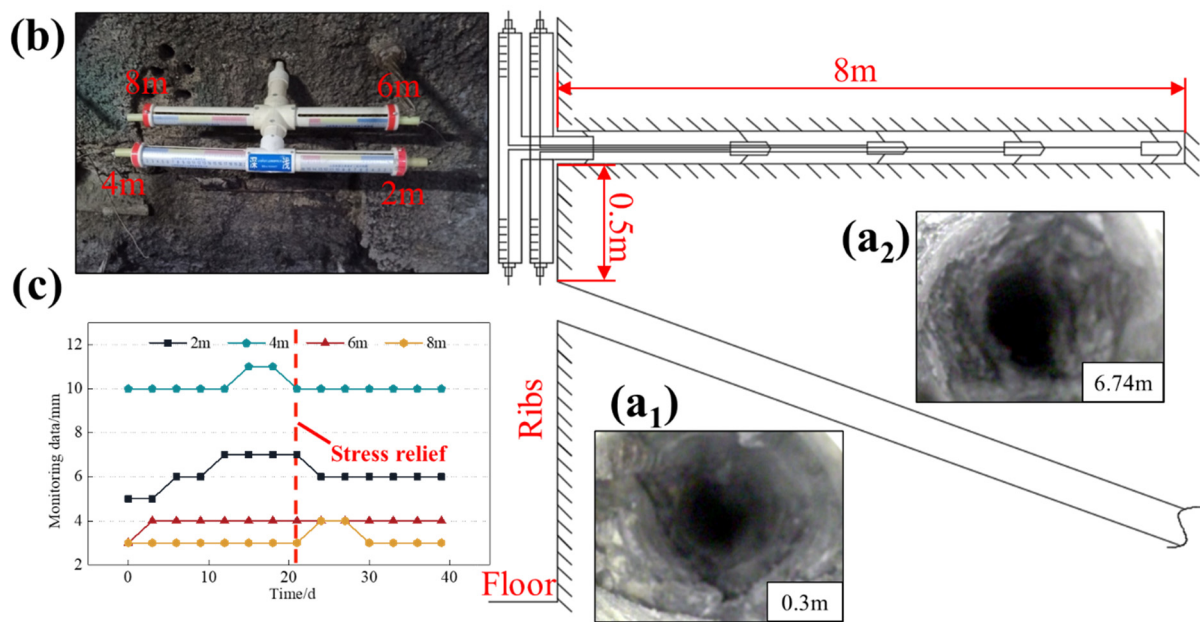


Figure 19. Deep displacement of roadway's surrounding rock. (a₁) Borehole peep image at 0.3 m; (a₂) Borehole peep image at 6.74 m; (b) Multi-point extensometer; (c) Chart of deep displacement with time.

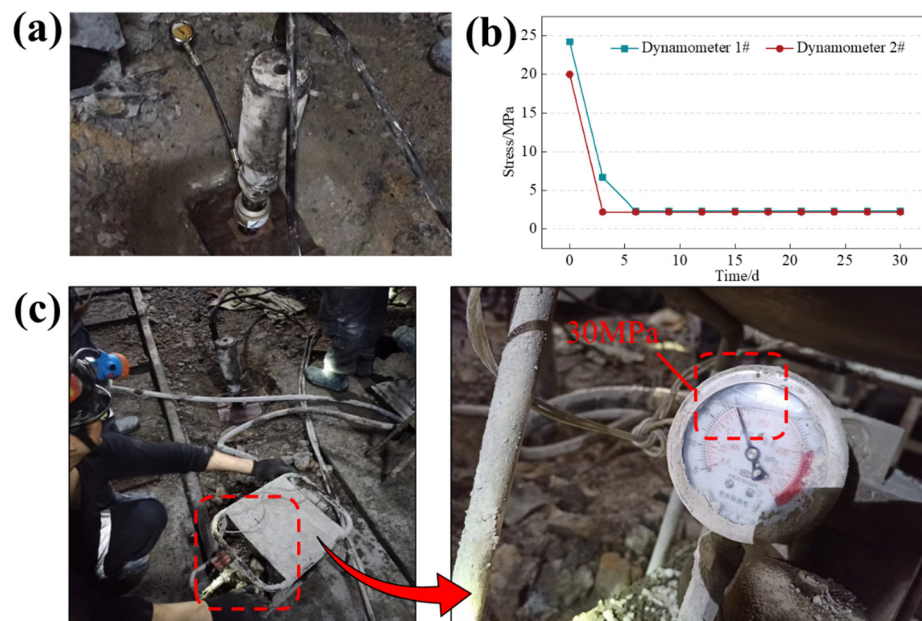


Figure 20. Working load of the anchor cable. (a) Instrument installation; (b) Diagram of stress variation of bolt with time; (c) Pull the anchor cable.

(2) Working load of the anchor cable. After the construction of the cables was completed, cable dynamometers were installed between the lock and the bearing plate, as shown in Figure 20a, to monitor the stress of the grouting cables on the floor. The stress monitoring curves of the anchor cable are shown in Figure 20b. It can be seen from the figure that the load responses of the 1# and 2# ergometer after the anchor cable was tensioned were 24.2 MPa and 20 MPa, respectively. With the diffusion of the tensioning prestress of the cable to the floor, the stress of the cable decreased to 2.3 MPa and 2.2 MPa, and then remained stable. During the whole observation period, no rebound of the cable was observed, and the cable was in good condition. The pull-out test of the floor cable conducted

to check the attenuation of the anchor cable's anchorage force is shown in Figure 20c. The results show that during the observation period, the pull-out force of the anchor cable was above 30 MPa (150 KN), and no anchoring failure phenomenon was observed.

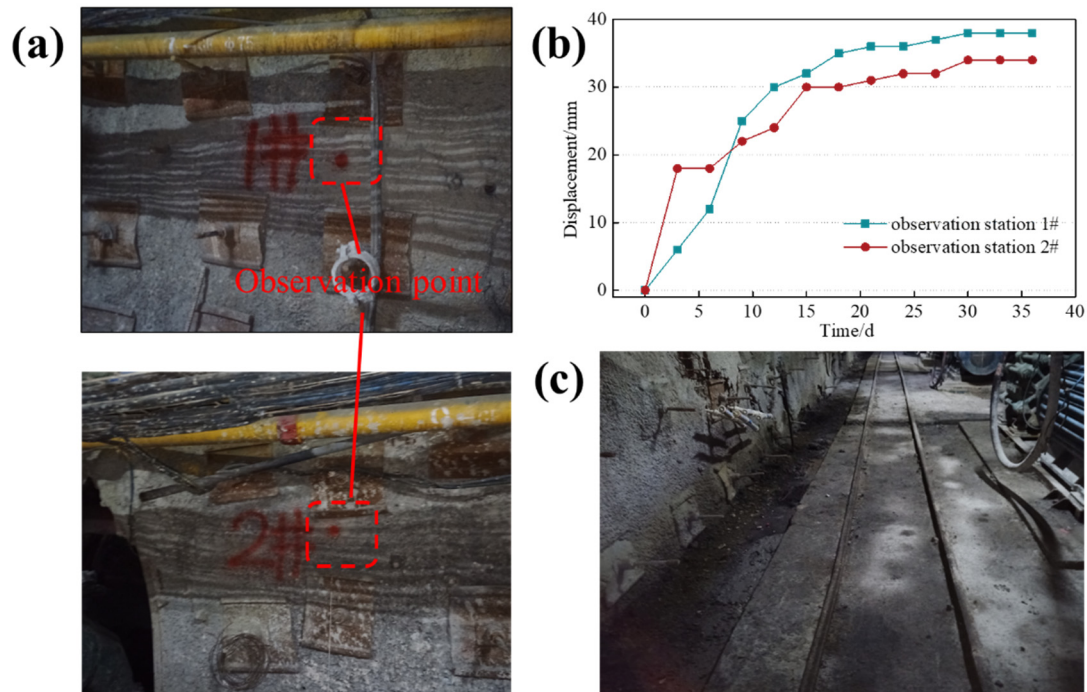


Figure 21. Roadway displacement. (a) Test site layout; (b) Chart of floor heave over time; (c) Tunnel floor at the end of the test.

(3) The roadway floor heave. As shown in Figure 21a, after the roadway support was completed and the concrete floor was poured, a floor deformation monitoring station was set up in the test area. The monitoring data of the test roadway floor heave are shown in Figure 21b. According to the analysis results, the extrusion floor heave was effectively controlled after the stress-relief–anchor-grouting collaborative control technology was adopted on the floor. The deformation of the roadway's floor mainly occurred within 15 days at the initial stage of excavation and then gradually became stable. Forty days after the excavation of the roadway, the deformations of the floor of the 1# and 2# measuring stations were only 38 mm and 34 mm, which is only 16.3% of that when the floor was not supported, achieving a good floor bulge control effect and ensuring the normal production of the mine.

6. Discussion

In the study, a laboratory test, in situ test, numerical simulation, and industrial test were used to study the control effect of borehole stress relief on deep roadway floor heave; the borehole parameters of stress relief were optimized; the floor-heave depression-anchor-injection collaborative control technology was developed; and the collaborative prevention and control of deep stress-extrusion floor heave was realized in three respects, stress, lithology, and support, to provide a new method for the floor heave control of deep roadway.

At present, the common floor-heave-control methods mainly include grouting reinforcement and strong anchorage. In contrast, the effect of the stress environment on the floor heave of the roadway was considered in the study. Based on the previous research results, the authors tried to apply the borehole stress-relief technology to control of the two ribs' extrusion deformation in the gravity stress field. The application of floor heave control not only validates the previous results but also solves the problem of large deformation

of a deep roadway floor. However, it should be noted that the determination of stress relief borehole parameters should fully consider factors such as the stress environment of roadways and the properties of surrounding rock, and the verification should be carried out strictly according to the production of geological conditions of the test roadway, so that the appropriate borehole parameter ranges are given to ensure that the roadway is in a state of full stress relief and to prevent the deformation from being difficult to control due to insufficient stress relief, or the roadway from becoming unstable due to excessive stress relief.

In addition, through a large number of data tests, the design sequence of stress-relief borehole parameters is optimized. Firstly, the borehole angle is determined according to the section size of the roadway and the direction of the principal stress; then, the borehole length is designed. Meanwhile, considering the correlation between diameter and row spacing, it is suggested that the two analyses be combined. For mines under similar conditions, the above sequence could be followed to optimize the design of pressure-relief borehole parameters. Finally, the large deformation of a deep roadway floor can be controlled significantly with the help of the current high-strength anchor injection technology.

7. Conclusions

Under the influence of high stress, deep roadways are prone to severe extrusion floor heave. Reducing the stress environment of the roadways' surrounding rock is an effective means to control extrusion floor heave. Based on laboratory tests and in situ stress tests, a control example of severe extrusion floor heave was analyzed in this study, and we obtained the following primary research results.

A directional stress-relief zone can be constructed using the borehole stress-relief technology, which can effectively cut off the stress transfer path and improve the stress environment of the floor while releasing stress. Based on the construction of the stress-relief belt, the control effects of the angle, length, diameter, and row spacing of stress-relief boreholes on the extrusion-type floor heave were studied via the numerical simulation method, and the reasonable thresholds of the borehole parameters were obtained to ensure the stress-relief effect. Combined with the specific conditions of the test roadway, the optimal combination of pressure relief parameters was determined, which were a borehole angle of 20°, a length of 14 m, a diameter of 113 mm, and a row distance of 350 mm; these parameters guided the construction of stress-relief boreholes in the field.

With the aim of ensuring the stress relief effect, the anchor-grouting technology was used to strengthen the support of the roadway floor, the broken surrounding rock of the floor was modified through the consolidation effect of the grouting, and the support stiffness of the floor was enhanced through the application of high prestress.

Based on the comprehensive consideration of stress regulation, the modification of surrounding rock, and the strengthening of the support, a stress-relief–anchor-grouting collaborative control technology of roadway floor heave based on borehole relief is presented in this study, which provides a new method for the severe extrusion floor heave control of deep roadways and has a good application value.

Author Contributions: Conceptualization, M.W. and D.L.; methodology, D.S.; software, D.S.; validation, D.S., C.Y. and S.H.; formal analysis, J.L., investigation, L.Z.; resources, C.Y.; data curation, S.W.; writing—original draft preparation, D.S.; writing—review and editing, D.S.; visualization, D.S.; supervision, M.W.; project administration, M.W.; funding acquisition, M.W. All authors have read and agreed to the published version of the manuscript.

Funding: This research was funded by the National Natural Science Foundation of China, grant number 52174074, Natural Science Foundation of Henan Province, grant number 222300420048, Science and Technology Innovation Talents in Universities of Henan Province, grant number 23HASTITO12, and Foundation for Distinguished Young Scientists of Henan Polytechnic University, grant number J2021-4.

Institutional Review Board Statement: Not applicable.

Informed Consent Statement: Not applicable.

Data Availability Statement: The data presented in this study are available in the article itself.

Acknowledgments: The authors wish to express their gratitude for the financial support that has made this study possible.

Conflicts of Interest: The authors declare no conflict of interest.

References

1. Xie, H.P.; Gao, M.Z.; Zhang, R.; Peng, G.Y.; Wang, W.Y.; Li, A.Q. Study on the Mechanical Properties and Mechanical Response of Coal Mining at 1000 m or Deeper. *Rock Mech. Rock Eng.* **2019**, *52*, 1475–1490. [[CrossRef](#)]
2. Kang, H.P.; Gao, F.P.; Xu, G.; Ren, H.W. Mechanical behaviors of coal measures and ground control technologies for China's deep coal mines—A review. *J. Rock Mech. Geotech. Eng.* **2023**, *15*, 37–65. [[CrossRef](#)]
3. Xie, H.P.; Lu, J.; Li, C.B.; Li, M.H.; Gao, M.Z. Experimental study on the mechanical and failure behaviors of deep rock subjected to true triaxial stress: A review. *Int. J. Min. Sci. Technol.* **2022**, *32*, 915–950. [[CrossRef](#)]
4. Wu, S.S.; Hao, W.Q.; Yao, Y.; Li, D.Q. Investigation into durability degradation and fracture of cable bolts through laboratorial tests and hydrogeochemical modelling in underground conditions. *Tunn. Undergr. Space Technol.* **2023**, *138*, 105198. [[CrossRef](#)]
5. Xie, H.P.; Li, C.; He, Z.Q.; Li, C.B.; Lu, Y.Q.; Zhang, R.; Gao, M.Z.; Gao, F. Experimental study on rock mechanical behavior retaining the in situ geological conditions at different depths. *Int. J. Rock Mech. Min.* **2021**, *138*, 104548. [[CrossRef](#)]
6. Jiang, Y.D.; Lu, S.L. Study on floor heave mechanism of roadway. *J. China Coal Soc.* **1994**, *4*, 343–351. [[CrossRef](#)]
7. Mo, S.; Ramandi, H.L.; Oh, J.; Masoumi, H.; Canbulat, I.; Hebblewhite, B.; Saydam, S. A new coal mine floor rating system and its application to assess the potential of floor heave. *Int. J. Rock Mech. Min.* **2020**, *128*, 104241. [[CrossRef](#)]
8. Mo, S.; Tutuk, K.; Saydam, S. Management of floor heave at Bulga Underground Operations—A case study. *Int. J. Min. Sci. Technol.* **2019**, *29*, 73–78. [[CrossRef](#)]
9. Mo, S.; Sheffield, P.; Corbett, P.; Ramandi, H.L.; Oh, J.; Canbulat, I.; Saydam, S. A numerical investigation into floor buckling mechanisms in underground coal mine roadways. *Tunn. Undergr. Space Technol.* **2020**, *103*, 103497. [[CrossRef](#)]
10. Kang, H.P.; Lu, S.L. Analysis of roadway floor heave mechanism. *Chin. J. Rock Mech. Eng.* **1991**, *4*, 362–373.
11. Zhu, Q.Z.; Li, T.C.; Zhang, H.; Ran, J.L.; Li, H.; Du, Y.T.; Li, W.T. True 3D geomechanical model test for research on rheological deformation and failure characteristics of deep soft rock roadways. *Tunn. Undergr. Space Technol.* **2022**, *128*, 104653. [[CrossRef](#)]
12. Jiang, Y.D.; Zhao, X.Y.; Liu, W.G.; Li, Q. Research on floor heave of roadway in deep mining. *Chin. J. Rock Mech. Eng.* **2004**, *23*, 2396–2401.
13. Tang, S.B.; Tang, C.A. Numerical studies on tunnel floor heave in swelling ground under humid conditions. *Int. J. Rock Mech. Min.* **2012**, *55*, 139–150. [[CrossRef](#)]
14. Wang, T.; Yan, C.Z.; Wang, G.; Zheng, Y.C.; Ke, W.H.; Jiao, Y.Y. Numerical study on the deformation and failure of soft rock roadway induced by humidity diffusion. *Tunn. Undergr. Space Technol.* **2022**, *126*, 104565. [[CrossRef](#)]
15. He, M.C.; Zhang, G.F.; Wang, G.L.; Xu, Y.L.; Wu, C.Z.; Tang, Q.D. Research on mechanism and application to floor heave control of deep gateway. *Chin. J. Rock Mech. Eng.* **2009**, *28*, 2593–2598.
16. Wang, W.J.; Feng, T. Study on mechanism of reinforcing sides to control floor heave of extraction opening. *Chin. J. Rock Mech. Eng.* **2005**, *5*, 808–811.
17. Li, X.H.; Wang, W.J.; Hou, C.J. Numerical analysis of floor heave controlled by roof reinforced. *J. China Univ. Min. Technol.* **2003**, *4*, 98–101.
18. Chen, Y.; Bai, J.B.; Yan, S.; Xu, Y.; Wang, X.Y.; Ma, S.Q. Control mechanism and technique of floor heave with reinforcing solid coal side and floor corner in gob-side coal entry retaining. *Int. J. Min. Sci. Technol.* **2012**, *22*, 841–845. [[CrossRef](#)]
19. Bai, J.B.; Li, W.F.; Wang, X.Y.; Xu, Y.; Huo, L.J. Mechanism of floor heave and control technology of roadway induced by mining. *J. Min. Saf. Eng.* **2011**, *28*, 1–5.
20. Zhang, D.; Bai, J.B.; Yan, S.; Wang, R.; Meng, N.K.; Wang, G.Y. Failure mechanism of surrounding rock and control of floor heave in heterogeneous composite rock roadway. *Chin. J. Rock Mech. Eng.* **2022**, *44*, 1699–1709+9–10.
21. Xu, Y.; Chen, J.; Bai, J.B. Control of floor heaves with steel pile in gob-side entry retaining. *Int. J. Min. Sci. Technol.* **2016**, *26*, 527–534. [[CrossRef](#)]
22. Zhao, Y.M.; Liu, N.; Zheng, X.G.; Zhang, N. Mechanical model for controlling floor heave in deep roadways with U-shaped steel closed support. *Int. J. Min. Sci. Technol.* **2015**, *25*, 713–720. [[CrossRef](#)]
23. Yang, R.S.; Zhu, Y.; Li, Y.L.; Li, W.Y. Floor heave mechanism and control measures of layered floor in weakly cemented soft rock roadway. *J. Min. Saf. Eng.* **2020**, *37*, 443–450. [[CrossRef](#)]
24. Yang, R.S.; Zhu, Y.; Li, Y.L.; Li, W.Y.; Xiao, B. Stability analysis and control strategy of weakly cemented layered floor in mining affected roadway. *J. China Coal Soc.* **2020**, *45*, 2667–2680. [[CrossRef](#)]
25. Sun, X.M.; Wang, D.; Feng, J.L.; Zhang, C.; Chen, Y.W. Deformation control of asymmetric floor heave in a deep rock roadway: A case study. *Int. J. Min. Sci. Technol.* **2014**, *24*, 799–804. [[CrossRef](#)]

26. Sun, X.M.; Chen, F.; He, M.C.; Gong, W.L.; Xu, H.C.; Lu, H. Physical modeling of floor heave for the deep-buried roadway excavated in ten degrees inclined strata using infrared thermal imaging technology. *Tunn. Undergr. Space Technol.* **2017**, *63*, 228–243. [[CrossRef](#)]
27. Sun, X.M.; Miao, P.Y.; Shen, F.X.; Zhao, W.C.; Yang, M.H. Study on floor heave mechanism of horizontal layered soft rock roadway in deep well under different stress states. *J. Min. Saf. Eng.* **2018**, *35*, 1099–1106. [[CrossRef](#)]
28. Wang, M.; Guo, G.L.; Wang, X.Y.; Guo, Y.; Dao, V. Floor heave characteristics and control technology of the roadway driven in deep inclined-strata. *Int. J. Min. Sci. Technol.* **2015**, *25*, 267–273. [[CrossRef](#)]
29. Wang, Z.Q.; Wang, P.; Lv, W.Y.; Shi, L.; Su, Z.H.; Wu, C.; Yu, F. Mechanism and control of asymmetric floor heave in gob-side entry. *J. Min. Saf. Eng.* **2021**, *38*, 215–226. [[CrossRef](#)]
30. Cheng, J.Y.; Wei, Z.J.; Bai, J.C.; Yu, Z.Z.; Xing, K.K.; Li, Q.M.; Wang, J.Y.; Li, X.; Zhang, C.; Zhang, Z.J. Study on floor heave control technology of deep tectonic stress water-rich soft rock roadway based on blasting pressure relief. *Coal Sci. Technol.* **2022**, *50*, 117–126. [[CrossRef](#)]
31. Sun, L.H.; Yang, B.S.; Sun, C.D.; Li, X.; Wang, C.W. Experimental research on mechanism and controlling of floor heave in deep soft rock roadway. *J. Min. Saf. Eng.* **2017**, *34*, 235–242. [[CrossRef](#)]
32. Wang, X.Q.; Kan, J.G.; Jiao, J.K. Mechanism of floor heave in the roadway with high stress and soft rock and its control practice. *J. Min. Saf. Eng.* **2017**, *34*, 214–220+227. [[CrossRef](#)]
33. Wang, J.; Guo, Z.B.; Yan, Y.B.; Pang, J.W.; Zhao, S.J. Floor heave in the west wing track haulage roadway of the Tingnan Coal Mine: Mechanism and control. *Int. J. Min. Sci. Technol.* **2012**, *22*, 295–299. [[CrossRef](#)]
34. Chang, Q.L.; Zhou, H.Q.; Xie, Z.H.; Shen, S.P. Anchoring mechanism and application of hydraulic expansion bolts used in soft rock roadway floor heave control. *Int. J. Min. Sci. Technol.* **2013**, *23*, 323–328. [[CrossRef](#)]
35. Hou, C.J. *Roadway Surrounding Rock Control*; China University of Mining and Technology Press: Xuzhou, China, 2013.
36. Zhang, J.F.; Jiang, F.X.; Yang, J.B.; Bai, W.S.; Zhang, L. Rockburst mechanism in soft coal seam within deep coal mines. *Int. J. Min. Sci. Technol.* **2017**, *27*, 551–556. [[CrossRef](#)]
37. Zhang, W.; Gu, S.T.; Sun, W.F.; Zhang, Q.; Gu, Q.H.; Jia, G.Y. Optimization study on pressure relief gateway layout for fully—Mechanized top coal caving mining with gateway driven along goaf. *J. China Univ. Min. Technol.* **2017**, *45*, 34–38.
38. Yin, W.; Miao, X.X.; Zhang, J.X.; Zhong, S.J. Mechanical analysis of effective pressure relief protection range of upper protective seam mining. *Int. J. Min. Sci. Technol.* **2017**, *27*, 537–543. [[CrossRef](#)]
39. He, J.; Cao, L.T.; Wu, J.H.; Wang, B.S. Pressure relief parameters of floor slotting in roadway with rock burst hazards. *J. Min. Saf. Eng.* **2021**, *38*, 963–971. [[CrossRef](#)]
40. Kang, H.P. *Mechanism and Prevention of Floor Heave in Soft Rock Roadway*; Coal Industry Press: Beijing, China, 1993.
41. Li, G.C.; Yang, S.; Sun, Y.T.; Xu, J.W.; Li, Q.H. Research progress of roadway surrounding strata rock control technologies under complex conditions. *J. China Univ. Min. Technol.* **2022**, *50*, 29–45.
42. Wang, M.; Wang, X.Y.; Xiao, T.Q. Borehole destressing mechanism and determination method of its key parameters in deep roadway. *J. China Coal Soc.* **2017**, *42*, 1138–1145.
43. Chen, T. Principle and parameters optimization of energy release from anti-scour borehole in coal roadway floor. *Coal Sci. Technol.* **2023**, *51*, 21–31.
44. Liu, H.G.; He, Y.N.; Xu, J.H.; Han, L.J. Numerical simulation and industrial test of boreholes destressing technology in deep coal tunnel. *J. China Coal Soc.* **2007**, *148*, 33–37.
45. Wang, H.S.; Li, S.G.; Shuang, H.Q.; Du, Z.X.; You, L.D.; Liu, L. Pressure-relief gas drainage technique by high level borehole in lateral high drainage roadway. *J. Cent. South Univ.* **2016**, *47*, 1319–1326.
46. Cicek, S.; Tulu, I.B.; Dyke, V.M.; Klemetti, T.; Wickline, J. Application of the coal mine floor rating (CMFR) to assess the floor stability in a Central, Appalachian Coal Mine. *Int. J. Min. Sci. Technol.* **2021**, *31*, 83–89. [[CrossRef](#)] [[PubMed](#)]
47. Cao, P.; Li, H.Y.; Zhong, Y.F.; Wang, F. Mechanism and control of floor heave of deep buried roadway with high lateral pressure coefficient. *J. Cent. South Univ.* **2017**, *48*, 457–464.
48. Fu, M.X.; Liu, S.W.; Jia, H.S.; Zhang, W.G. Generation mechanism and size characteristics of the rock fragments during borehole drilling in coal mine roadway floor. *J. China Univ. Min. Technol.* **2021**, *50*, 228–238.
49. Wang, J.; Hao, Y.J.; Guo, Z.B.; Zhu, G.L.; Han, Z. Floor heave mechanism and control technology for east rail roadway of Tingnan coal mine. *J. Min. Saf. Eng.* **2015**, *32*, 291–297.
50. Hua, X.Z.; Yang, M.; Liu, Q.J.; Yang, P. Model test on evolution mechanism of floor heave in gob-side retainingentry of deep mine. *J. Min. Saf. Eng.* **2015**, *35*, 1–9.
51. Chang, J.C.; He, L.P. A research on cable supporting and curtain grouting of hydraulic hosecontrolling the roadway floor heave in deep coal mine. *J. Min. Saf. Eng.* **2015**, *32*, 968–972.
52. Fu, M.; Huang, S.; Liu, S.; Jia, H. Experimental Study on the Size of Rock Fragments Ejected from Boreholes Drilled in Coal Mine Roadway Floors. *Minerals* **2023**, *13*, 392. [[CrossRef](#)]
53. Meng, X.Y.; Cheng, D.Q.; Gou, P.F.; Li, S.B. Study on drilling release pressure parameters of gateway in “three soft” coal seam. *J. Henan Poly. Univ.* **2011**, *30*, 529–533.
54. Gai, D.C.; Li, D.; Jiang, F.X.; Wang, C.W.; Chen, Y.; Dong, C.Y.; Sun, S.H.; Yang, G.G. Reasonable pressure-relief borehole spacing in coal of different strength. *J. Min. Saf. Eng.* **2020**, *37*, 578–585+593.

55. Peng, J.; Cai, M.; Rong, G.; Yao, M.D.; Jiang, Q.H.; Zhou, C.B. Determination of confinement and plastic strain dependent post-peak strength of intact rocks. *Eng. Geol.* **2017**, *218*, 187–196. [[CrossRef](#)]
56. Zhao, H.; Zhang, C.; Cao, W.G.; Zhao, M.H. Statistical meso-damage model for quasi-brittle rocks to account for damage tolerance principle. *Environ. Earth Sci.* **2016**, *75*, 862. [[CrossRef](#)]
57. Zhang, K.; Liu, C.Y.; Zhang, H.R.; Yue, X.; Liu, H.D. Research on Roof Cutting Pressure Relief of the Gob-Side Entry Retaining with Roadside Backfilling. *Front. Earth Sci.* **2022**, *10*, 835497. [[CrossRef](#)]
58. Chen, M.; Zhang, Y.L.; Zang, C.W.; Zhang, G.C.; Li, Q.; Jiang, B.Z. Experimental Investigation on Pressure Relief Mechanism of Specimens with Prefabricated Reaming Boreholes. *Rock Mech. Rock Eng.* **2023**, *56*, 2949–2966. [[CrossRef](#)]
59. Meng, N.K.; Bai, J.B.; Yoo, C. Failure mechanism and control technology of deep soft-rock roadways: Numerical simulation and field study. *Undergr. Space* **2023**, *12*, 1–17. [[CrossRef](#)]
60. Freudenthal, T.; Villinger, H.; Riedel, M.; Pape, T. Heat flux estimation from borehole temperatures acquired during logging while tripping: A case study with the sea floor drill rig MARUM-MeBo. *Mar. Geophys. Res.* **2022**, *43*, 37. [[CrossRef](#)]
61. Kang, Y.S.; Liu, Q.S.; Gong, G.Q.; Wang, H.C. Application of a combined support system to the weak floor reinforcement in deep underground coal mine. *Int. J. Rock Mech. Min. Sci.* **2014**, *71*, 143–150. [[CrossRef](#)]
62. Zhao, C.X.; Li, Y.M.; Liu, G.; Meng, X.R. Mechanism analysis and control technology of surrounding rock failure in deep soft rock roadway. *Eng. Fail. Anal.* **2020**, *115*, 104611. [[CrossRef](#)]

Disclaimer/Publisher’s Note: The statements, opinions and data contained in all publications are solely those of the individual author(s) and contributor(s) and not of MDPI and/or the editor(s). MDPI and/or the editor(s) disclaim responsibility for any injury to people or property resulting from any ideas, methods, instructions or products referred to in the content.